Science, Engineering and Technology Vol. 3, No. 1, pp. 36-46
www.setjournal.com https://doi.org/10.54327/set2023/v3.i2.68

Inclined MHD Effects in Tapered Asymmetric Porous Channel with Peristalsis: Applications in Biomedicine

Anum Tanveer, Sharak Jarral

Department of Mathematics, Mirpur University of Science and Technology (MUST), Mirpur 10250, AJK, Pakistan

Abstract

This paper emphasized an inclined magnetohydrodynamics (MHD) effects in tapered asymmetric porous channel with peristalsis in the presence of slip boundary conditions. Here we considered the two-dimensional channel with a porous medium. The fundamental assumptions of long wavelength and low Reynolds number are applied in the relevant nonlinear equations for momentum, heat, and mass transfer as part of mathematical modeling. The equations subjected to slip boundary conditions have been solved numerically by the Mathematica software. Various essential physical characteristics of velocity, temperature, concentration, and heat transfer rate are captured graphically in the end. The velocity profile is found parabolic for various involved parameters. It is observed that the embedded parameters behave in the exact opposite manner when compared with temperature and concentration distributions. The sinusoidal behavior of the heat transfer rate is also displayed. The unique aspect of this effort is specifically to relate the Joule heating, Darcy resistance, and inclined magnetic field effects in peristaltic flow for a non-Newtonian Jeffrey fluid in an asymmetric tapered channel under the influence of slip boundary conditions. Such preferences have a wide range of applications in engineering, biology, and industry. The outcomes of the presented work are also proficient in the medical field for the treatment of cancer using MHD. The MHD also aids in controlling blood pressure during systolic and diastolic pressure conditions by regulating the blood flow stream.

Keywords: *peristalsis, inclined MHD, Jeffrey nanofluid, porous medium, asymmeteic tapered channel*

1. Introduction

Magnetohydrodynamics is the study of the magnetic properties and behavior of electrically conducting fluids. Medical sciences and advanced biomedical engineering are progressively studying magnetohydrodynamics (MHD) that has frequent applications in both engineering and medical fields. The MHD is predominantly utilized in the cancer treatment, hypothermia and open wounds in the medical industry. MHD effects are also employed to study electrolytes, plasma, hot metals and saltwater. Physiological applications of magnetic devices and magnetic particles include drug transfers and magnetic resonance imaging. Today, the brochure on MHD peristaltic transport of non-Newtonian fluids in a variety of geometries is vast. Some helpful studies on MHD are covered in the references [1-9].

The Greek term "Peristaltikos" originates the word "peristalsis" meaning contraction and expansion. The topic of peristalsis for viscous fluids is first executed by Latham [10]. Under long wavelength and low Reynolds number the peristalsis of viscous fluid has been examined by Shapiro et al. [11]. Due to its numerous uses in the fields of engineering and medicine, peristaltic transport is now the most exquisite topic in the scientific world. In biological systems, peristalsis is used for the movement of lymphatic vessels, capillary vasomotion and blood circulation in the arteries from

Corresponding author: Anum Tanveer *(anum.maths@must.edu.pk)*
Received: *3 February 2023*; Revised: *2 May 2023*; Accepted: *3 May 2023*; Published: 9 *May 2023*

heart pumping. The references [12-19] discuss a few insightful studies on peristalsis.

Non-Newtonian fluid plays a significant role in engineering and technology such as chemical industries, biological sciences and geophysics. Various types of non-Newtonian fluids including oils, ketchup, honey, paints and toothpaste are used in everyday activities. Due to numerous uses of non-Newtonian fluids in industries the peristaltic flow of these fluids cannot be neglected. Non-Newtonian fluids perform better computation when examining the rheology of naturally occurring processes. One of the non-Newtonian fluids is Jeffrey fluid that is found to give better relevance for physiological fluids. Such as describing blood flow in arteries. It is revealed that Jeffrey model is one of the significant non-Newtonian model which precise the best representation of viscoelastic fluids. The references [20-31] carry out some investigations regarding the use of Jeffrey liquid.

The impact of heat and mass transport has a variety of uses in the biomedical field. Numerous technological applications observed mass transfer in action in addition to heat transfer. In chemical engineering mass transfer is vital notably in chemical reactors and industrial operations. Convection is the most effective way to describe how heat is moved from one point to another during peristaltic flow through porous media in cryotherapy. Conduction, convection and radiation are the basic three ways that transfer heat in multiple systems. Evaluation of skin irritation, hypertension, the eradication of harmful cancer cells, the dilution technique for assessing blood flow and paper manufacturing is just a few of the plethora of processes that are involved in heat transmission. The references [32-43] cover some useful studies in heat and mass transfer.

The objective of this research is to construct a mathematical model to evaluate the consequences of inclined MHD along peristaltic channel. Jeffrey nanofluid in a tapered asymmetric channel with porous media has been considered in flow analysis. In our research the combined investigation of inclined asymmetric porous channel, slip boundary conditions, Darcy resistance, sloped MHD with peristaltic flow of non-Newtonian Jeffrey fluid is taken into account. In the realm of research, our paper is extremely innovative. This study intends to look into how velocity, temperature and concentration are affected by magnetic field and gravity in porous media. In order to simplify the resulting mathematical problem, the long-wavelength and low Reynolds number approximation are employed. The physical properties of emergent components are discussed by plotting their graphs in terms of velocity, temperature, concentration and heat transfer rate.

2. Mathematical Formulation

Consider a two dimensional inclined tapered asymmetric porous channel through which the Jeffrey nanofluid is flowing under peristaltic wave in the presence of magnetic field. The lower and upper walls are located at positions $Y = H_1$ and $Y = H_2$ with T_1, C_1 *and* T_0, C_0 the temperature and concentration of upper and lower walls respectively (see Figure 1) as follows.

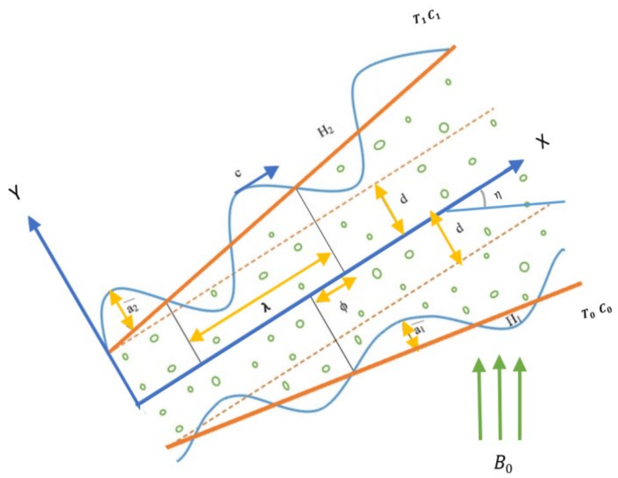

Figure 1. Geometrical demonstration of problem.

The geometry of walls is characterized by the subsequent form [31].

$$H_1 = -d - \overline{K_1}\bar{x} - \overline{a_1}\sin\left[\frac{2\pi}{\lambda}(\bar{x} - c\bar{t}) + \phi\right], \quad (1a)$$

$$H_2 = d + \overline{K_1}\bar{x} + \overline{a_2}\sin\left[\frac{2\pi}{\lambda}(\bar{x} - c\bar{t})\right]. \quad (1b)$$

Here d shows half width of the channel, λ is wavelength, $\bar{a}_1$ and $\bar{a}_2$is wave amplitude of lower and upper wall respectively,$\bar{t}$ denotes the timeand ϕshows the phase angle. We enforce uniform magnetic field which is [44-45].

$$\bar{B} = (0, 0, B_0 sin\,\eta), \quad (2)$$

by generalized Ohm's law

$$\bar{J} = \sigma\left[(\bar{E} + \bar{V} \times \bar{B}) - \frac{1}{en_e}(\bar{J} \times \bar{B})\right], \quad (3)$$

where $\bar{V}$ is fluid velocity, $\bar{J}$ the current density,σ the electrical conductivity and we disregarded the impact of the electric force, $\bar{E} = 0$. By using Eq. (2) and (3), we obtain:

$$\bar{J} \times \bar{B} = \frac{\sigma B_0^2 \sin^2\eta}{1+m^2\sin^2\eta}[(-\bar{U} + m\bar{V}\sin\eta)i - (\bar{V} + m\bar{U}\sin\eta)j + 0k]. \quad (4)$$

where $m = \frac{\sigma B_0}{en_e}$ represents the Hall current parameter.

Joule heating is listed below [34]:

$$\frac{\bar{J}.\bar{J}}{\sigma} = \frac{\sigma B_0^2 \sin^2\eta}{1+m^2\sin^2\eta}[\bar{U} + \bar{V}]. \quad (5)$$

The following equation describes the Cauchy stress tensor and extra stress tensor T and S for an incompressible Jeffrey material [36].

$$T = -PI + S, \quad (6)$$

$$S = \frac{\mu}{1+\lambda_1}\left(\dot{\gamma} + \lambda_2\frac{d\dot{\gamma}}{dt}\right). \quad (7)$$

The Rivilin-Ericksen tensor $\dot{\gamma}$ is listed below [19]

$$\dot{\gamma} = (\nabla\bar{V}) + (\nabla\bar{V})^t.$$

In term of Jeffrey fluid model, the Darcy resistance is [13]

$$R = -\frac{\mu}{k_1(1+\lambda_1)}\left(1 + \lambda_2\frac{d}{dt}\right)\bar{V}. \quad (8)$$

where $\bar{V}$ represent the fluid's velocity and k_1 the permeability parameter.

The flow of an incompressible nanofluid in a fixed frame is represented by the following equations [6]:

$$\frac{\partial\bar{U}}{\partial\bar{X}} + \frac{\partial\bar{V}}{\partial\bar{Y}} = 0, \quad (9)$$

$$\rho_f\left[\frac{\partial\bar{U}}{\partial\bar{t}} + \bar{U}\frac{\partial\bar{U}}{\partial\bar{X}} + \bar{V}\frac{\partial\bar{U}}{\partial\bar{Y}}\right] = -\frac{\partial\bar{P}}{\partial\bar{X}} + \frac{\partial}{\partial\bar{X}}(\bar{S}_{\overline{XX}}) + \frac{\partial}{\partial\bar{Y}}(\bar{S}_{\overline{XY}}) + (1 - C_0)\rho_f g\beta_t(\bar{T} - T_0) + \left(\frac{\rho_p - \rho_f}{\rho_f}\right)g\beta_c(\bar{C} - C_0) - \frac{\sigma B_0^2\sin^2\eta}{1+m^2\sin^2\eta}(\bar{U} - m\bar{V}\sin\eta) - \frac{\mu}{k_1(1+\lambda_1)}\left(\bar{U} + \lambda_2\frac{d\bar{U}}{dt}\right) + \rho_f g\sin\eta, \quad (10)$$

$$\rho_f\left[\frac{\partial\bar{V}}{\partial\bar{t}} + \bar{U}\frac{\partial\bar{V}}{\partial\bar{X}} + \bar{V}\frac{\partial\bar{V}}{\partial\bar{Y}}\right] = -\frac{\partial\bar{P}}{\partial\bar{Y}} + \frac{\partial}{\partial\bar{X}}(\bar{S}_{\overline{XY}}) + \frac{\partial}{\partial Y}(\bar{S}_{\overline{YY}}) - \frac{\sigma B_0^2\sin^2\eta}{1+m^2\sin^2\eta}(\bar{V} + m\bar{U}\sin\eta) - \frac{\mu}{k_1(1+\lambda_1)}\left(\bar{V} + \lambda_2\frac{d\bar{V}}{dt}\right) - \rho_f g\cos\eta, \quad (11)$$

$$\left[\frac{\partial\bar{T}}{\partial\bar{t}} + \bar{U}\frac{\partial\bar{T}}{\partial\bar{X}} + \bar{V}\frac{\partial\bar{T}}{\partial\bar{Y}}\right] = \alpha\left(\frac{\partial^2\bar{T}}{\partial\bar{X}^2} + \frac{\partial^2\bar{T}}{\partial\bar{Y}^2}\right) + \frac{1}{\rho_f c_f}\left[\bar{S}_{\overline{XX}}\frac{\partial\bar{U}}{\partial\bar{X}} + \bar{S}_{\overline{XY}}\left(\frac{\partial\bar{U}}{\partial\bar{Y}} + \frac{\partial\bar{V}}{\partial\bar{X}}\right) + \bar{S}_{\overline{YY}}\frac{\partial\bar{V}}{\partial\bar{Y}}\right] + \tau\left[D_B\left(\frac{\partial\bar{C}}{\partial\bar{X}}\frac{\partial\bar{T}}{\partial\bar{X}} + \frac{\partial\bar{C}}{\partial\bar{Y}}\frac{\partial\bar{T}}{\partial\bar{Y}}\right) + \frac{D_T}{T_m}\left(\left(\frac{\partial\bar{T}}{\partial\bar{X}}\right)^2 + \left(\frac{\partial\bar{T}}{\partial\bar{Y}}\right)^2\right)\right] + \frac{1}{\rho_f c_f}\frac{\sigma B_0^2\sin^2\eta}{1+m^2\sin^2\eta}[\bar{U}^2 + \bar{V}^2], \quad (12)$$

$$\left[\frac{\partial\bar{C}}{\partial\bar{t}} + \bar{U}\frac{\partial\bar{C}}{\partial\bar{X}} + \bar{V}\frac{\partial\bar{C}}{\partial\bar{Y}}\right] = D_B\left(\frac{\partial^2\bar{C}}{\partial\bar{X}^2} + \frac{\partial^2\bar{C}}{\partial\bar{Y}^2}\right) + \frac{D_T}{T_m}\left(\frac{\partial^2\bar{T}}{\partial\bar{X}^2} + \frac{\partial^2\bar{T}}{\partial\bar{Y}^2}\right). \quad (13)$$

The frame $(\bar{x}, \bar{y})$ in which the flow is thought to be steady is flowing at a velocity of c. The transformations between the laboratory and wave frame are [6]:

$$\bar{x} = \bar{X} + c\bar{t},\ \bar{y} = \bar{Y},\ \bar{u} = \bar{U} - c,\ \bar{v} = \bar{V},\ \bar{p}(\bar{x}, \bar{y}) = \bar{P}(\bar{X}, \bar{Y}, \bar{t}),\ T = \bar{T}. \quad (14)$$

$$x = \frac{\bar{x}}{\lambda},\ y = \frac{\bar{y}}{d},\ u = \frac{\bar{u}}{c},\ v = \frac{\bar{v}}{c},\ t = \frac{c\bar{t}}{\lambda},\ a_1 = \frac{\overline{a_1}}{d},$$

$$a_2 = \frac{\overline{a_2}}{d},\ \delta = \frac{d}{\lambda}, h_1 = \frac{\overline{H_1}}{d}, h_2 = \frac{\overline{H_2}}{d},\ v = \frac{\mu}{\rho_f}, k_1 = \frac{\lambda\overline{k_1}}{d},$$

$$p = \frac{d^2\bar{p}}{c\lambda\mu},\ M = \sqrt{\frac{\sigma}{\mu}}B_0 d,\ \overline{\lambda_2} = \frac{\lambda_2\, c}{d},\ Pr = \frac{v}{\alpha},\ Re =$$

$\frac{cd}{v}$, $S=\frac{\bar{S}d}{\mu c}$, $Gm=\frac{(\rho_c-\rho_f)g\beta_c(C_1-C_0)d^2}{\mu c}$, $Nt=\frac{\tau D_T(T_1-T_0)}{vT_m}$, $Nb=\frac{\tau D_B(C_1-C_0)}{v}$, $Br=Pr\times Ec$, $Fr=\frac{c^2}{gd}$, $Da=\frac{k_1}{d^2}$, $Gr=\frac{(1-C_0)\rho_f g\beta_t(T_1-T_0)d^2}{\mu c}$, $Ec=\frac{c^2}{c_f(T_1-T_0)}$, $\theta=\frac{\bar{T}-T_0}{T_1-T_0}$, $\zeta=\frac{\bar{C}-C_0}{C_1-C_0}$ (15)

3. Solution to Problem

After using dimensionless variables (15) and falling bars, the Eqs. (10-13) become:

$$Re\delta\left[(u+1)\frac{\partial u}{\partial x}+\frac{v}{\delta}\frac{\partial u}{\partial y}\right]=-\frac{\partial p}{\partial x}+\delta\frac{\partial}{\partial x}(S_{xx})+\frac{\partial}{\partial y}(S_{xy})+Gr\theta+Gm\zeta-\frac{M^2\sin^2\eta}{1+m^2\sin^2\eta}(u+1)+\frac{M^2\sin^2\eta}{1+m^2\sin^2\eta}(mv\sin\eta)-\frac{1}{D_a(1+\lambda_1)}\left(1+\frac{c\lambda_2}{d}\left(\delta\frac{\partial u}{\partial x}+\frac{\partial v}{\partial y}\right)\right)\times(u+1)+\frac{Re}{Fr}\sin\eta\,, \tag{16}$$

$$Re\delta^2\left[(u+1)\frac{\partial v}{\partial x}+\frac{v}{\delta}\frac{\partial v}{\partial y}\right]=-\frac{\partial p}{\partial y}+\delta^2\frac{\partial}{\partial x}(S_{xy})+\delta\frac{\partial}{\partial y}(S_{yy})-\delta v\left(\frac{M^2\sin^2\eta}{1+m^2\sin^2\eta}\right)-\delta\left(\frac{M^2\sin^2\eta}{1+m^2\sin^2\eta}\right)m\sin\eta\times(u+1)-\frac{\delta v}{D_a(1+\lambda_1)}\left(1+\frac{c\lambda_2}{d}\left(\delta\frac{\partial u}{\partial x}+\frac{\partial v}{\partial y}\right)\right)-\delta\frac{Re}{Fr}\cos\eta, \tag{17}$$

$$\left[(u+1)\frac{\partial\theta}{\partial x}+\frac{v}{\delta}\frac{\partial\theta}{\partial y}\right]=Ec\left[\delta S_{xx}\frac{\partial u}{\partial x}+S_{xy}\left(\frac{\partial u}{\partial y}+\delta^2\frac{\partial v}{\partial x}\right)+S_{yy}\frac{\partial v}{\partial y}+\frac{M^2\sin^2\eta}{1+m^2\sin^2\eta}((u+1)^2+v^2)\right]+\frac{1}{Pr}\left[\delta^2\frac{\partial^2\theta}{\partial x^2}+\frac{\partial^2\theta}{\partial y^2}\right]+Nb\left[\delta^2\frac{\partial\theta}{\partial x}\frac{\partial\zeta}{\partial x}+\frac{\partial\theta}{\partial y}\frac{\partial\zeta}{\partial y}\right]+\left[\delta^2\left(\frac{\partial\theta}{\partial x}\right)^2+\left(\frac{\partial\theta}{\partial y}\right)^2\right], \tag{18}$$

$$Re\delta\left[(u+1)\frac{\partial\zeta}{\partial x}+\frac{v}{\delta}\frac{\partial\zeta}{\partial y}\right]=\left(\delta^2\frac{\partial^2\zeta}{\partial x^2}+\frac{\partial^2\zeta}{\partial y^2}\right)+\frac{Nt}{Nb}\left(\delta^2\frac{\partial^2\theta}{\partial x^2}+\frac{\partial^2\theta}{\partial y^2}\right), \tag{19}$$

The stream function and designated velocity fields are now being inserted.

$$u=\frac{\partial\psi}{\partial y},\ v=-\delta\frac{\partial\psi}{\partial x}. \tag{20}$$

where the stress elements are represented by the following form:

$$S_{xx}=\frac{2\delta}{(1+\lambda_1)}\left[1+\frac{\lambda_2 c\delta}{d}\left(\psi_y\frac{\partial}{\partial x}-\psi_x\frac{\partial}{\partial y}\right)\right]\psi_{xy}, \tag{21}$$

$$S_{xy}=\frac{1}{(1+\lambda_1)}\left[1+\frac{\lambda_2 c\delta}{d}\left(\psi_y\frac{\partial}{\partial x}-\psi_x\frac{\partial}{\partial y}\right)\right](\psi_{yy}-\delta^2\psi_{xx}), \tag{22}$$

$$S_{yy}=-\frac{2\delta}{(1+\lambda_1)}\left[1+\frac{\lambda_2 c\delta}{d}\left(\psi_y\frac{\partial}{\partial x}-\psi_x\frac{\partial}{\partial y}\right)\right]\psi_{xy}. \tag{23}$$

Using the preceding non-dimensional governing flow Eqs. (16)-(19) with long wavelengths and low Reynolds number approximations one gets

$$0=-\frac{\partial p}{\partial x}+\left(\frac{1}{1+\lambda_1}\right)\frac{\partial^3\psi}{\partial y^3}+Gr\theta+Gm\zeta-\left(\frac{M^2\sin^2\eta}{1+m^2\sin^2\eta}+\frac{1}{D_a(1+\lambda_1)}\right)\left[\frac{\partial\psi}{\partial y}+1\right]+\frac{Re}{Fr}\sin\eta, \tag{24}$$

$$0=-\frac{\partial p}{\partial y}\ , \tag{25}$$

$$0=\frac{\partial^2\theta}{\partial y^2}+Br\left[\left(\frac{1}{1+\lambda_1}\right)\left(\frac{\partial^2\psi}{\partial y^2}\right)^2+\frac{M^2\sin^2\eta}{1+m^2\sin^2\eta}\left(\frac{\partial\psi}{\partial y}+1\right)^2\right]+PrNb\frac{\partial\theta}{\partial y}\frac{\partial\zeta}{\partial y}+PrNt\left(\frac{\partial\theta}{\partial y}\right)^2, \tag{26}$$

$$0=\frac{\partial^2\zeta}{\partial y^2}+\frac{Nt}{Nb}\frac{\partial^2\theta}{\partial y^2}. \tag{27}$$

After abolishing the pressure gradient term Eqs. (24-25) reduce to subsequent form.

$$\left(\frac{1}{1+\lambda_1}\right)\frac{\partial^4\psi}{\partial y^4}+Gr\frac{\partial\theta}{\partial y}+Gm\frac{\partial\zeta}{\partial y}-\left(\frac{M^2\sin^2\eta}{1+m^2\sin^2\eta}+\frac{1}{D_a(1+\lambda_1)}\right)\frac{\partial^2\psi}{\partial y^2}=0, \tag{28}$$

The boundary conditions are defined as follows [24]:

$$\psi = \frac{q}{2},\ \frac{\partial\psi}{\partial y} + \alpha_1\left(\frac{1}{1+\lambda_1}\right)\frac{\partial^2\psi}{\partial y^2} = 0,\ \theta + \alpha_2\frac{\partial\theta}{\partial y} = 1,\ \zeta + \alpha_3\frac{\partial\zeta}{\partial y} = 1\ at\ y = h_2 = 1 + k_1 x + a_2\sin[2\pi(x-t)], \quad (29)$$

$$\psi = -\frac{q}{2},\ \frac{\partial\psi}{\partial y} - \alpha_1\left(\frac{1}{1+\lambda_1}\right)\frac{\partial^2\psi}{\partial y^2} = 0,\ \theta - \alpha_2\frac{\partial\theta}{\partial y} = 0,\ \zeta - \alpha_3\frac{\partial\zeta}{\partial y} = 0\ at\ y = h_1 = -1 - k_1 x - a_1\sin[2\pi(x-ct)+\phi]. \quad (30)$$

The wave and fixed frame's flow rates are related by [6]:

$$Q = q + 1 + d. \quad (31)$$

Dimensionless form of Heat transfer rate in is listed below [18].

$$Z = h_2{}'(x)\left|\frac{\partial\theta}{\partial y}\right|_{y=h_2}. \quad (32)$$

4. Numerical Method

By using the Mathematica ND solve technique, the modified dimensionless equations are numerically processed. The benefit of this approach is that it picks the right algorithm and detects any possible errors automatically. Furthermore, this technique delivers excellent computational output with just three to four minutes of CPU time required for each evaluation. In reality, this approach avoids complex solution expressions and directly displays graphical depictions. The Eqs, (26)-(28) subjected to boundary conditions (29) and (30) have been solved numerically by the ND_solve method. The commercial software Mathematica includes a built-in feature for validating the results. The governing equations (26-28) are coupled and have a significant degree of nonlinearity. It is impossible to find the exact solution. Consequently, the numerical solution has been obtained.

5. Result and Discussion

In this section, the effects of pertinent parameters on common profiles (concentration, temperature, and velocity) are discussed. In-depth discussion is held regarding the factors that affect the peristaltic transport of a nanofluid, including Grashof number Gr($0.5 \le Gr \le 2.0$), Hartmann number M($0.0 \le M \le 3.0$), nanoparticle Grashof number Gm($0.5 \le Gm \le 2.0$), flow rates Q($4.0 \le Q \le 5.5$),the ratio of relaxation to retardation times λ_1 ($1.0 \le \lambda_1 \le 4.0$), Darcy number Da($0.3 \le Da \le 1.2$), Brinkman number Br($0.2 \le Br \le 1.4$), Brownian motion parameter Nb($0.2 \le Nb \le 0.8$), thermophoresis parameter Nt($0.2 \le Nt \le 0.8$), and Prandtl number Pr($0.5 \le Pr \le 2.0$). The numerical computation is performed using the Mathematica built-in numerical ND-Solve method.

The outlook of velocity profiles for variation in various involved parameters is parabolic. The velocity profile at the centre of the channel decays and the walls of the channel experiencing an opposite behaviour when M is increased (see Figure 2(a)). Dual responce of velocity is captured for rising values of Gm and Gr (see Figure 2(b) and Figure 2(c)). It depicted in Figure 2(d) as the value of Da increases, then the velocity distribution increases at central portion and dropped at the lower part of channel. Figure 2(e) corresponds to dual impact of λ_1 on velocity profile. As in Figure 2(f) the flow rate Q is elevated, the velocity distribution increases. Moreover, it is observed that the velocity profiles satisfy the boundary requirements. Our results for Figure 2(a) and Figure 2(d) are analogous to the outcomes reported in ref. [46].

In Figure 3(a) Temperature is seen to grow when the values ofpertinent parameters M boost.It is noticed that in Figure 3(b) the escalating values of the Brikmann number Br enhances the temperature profile owing to the effects of viscous dissipation. We noticed that Temperature rises up with the increament in the value of Nb and Nt (see Figure 3(c) and Figure 3(d)). These outcomes for temperature profile are appropriately matched with the results gained by Abd-Alla et al. [6]. The temperature distribution also appears to fulfill the boundary condition.

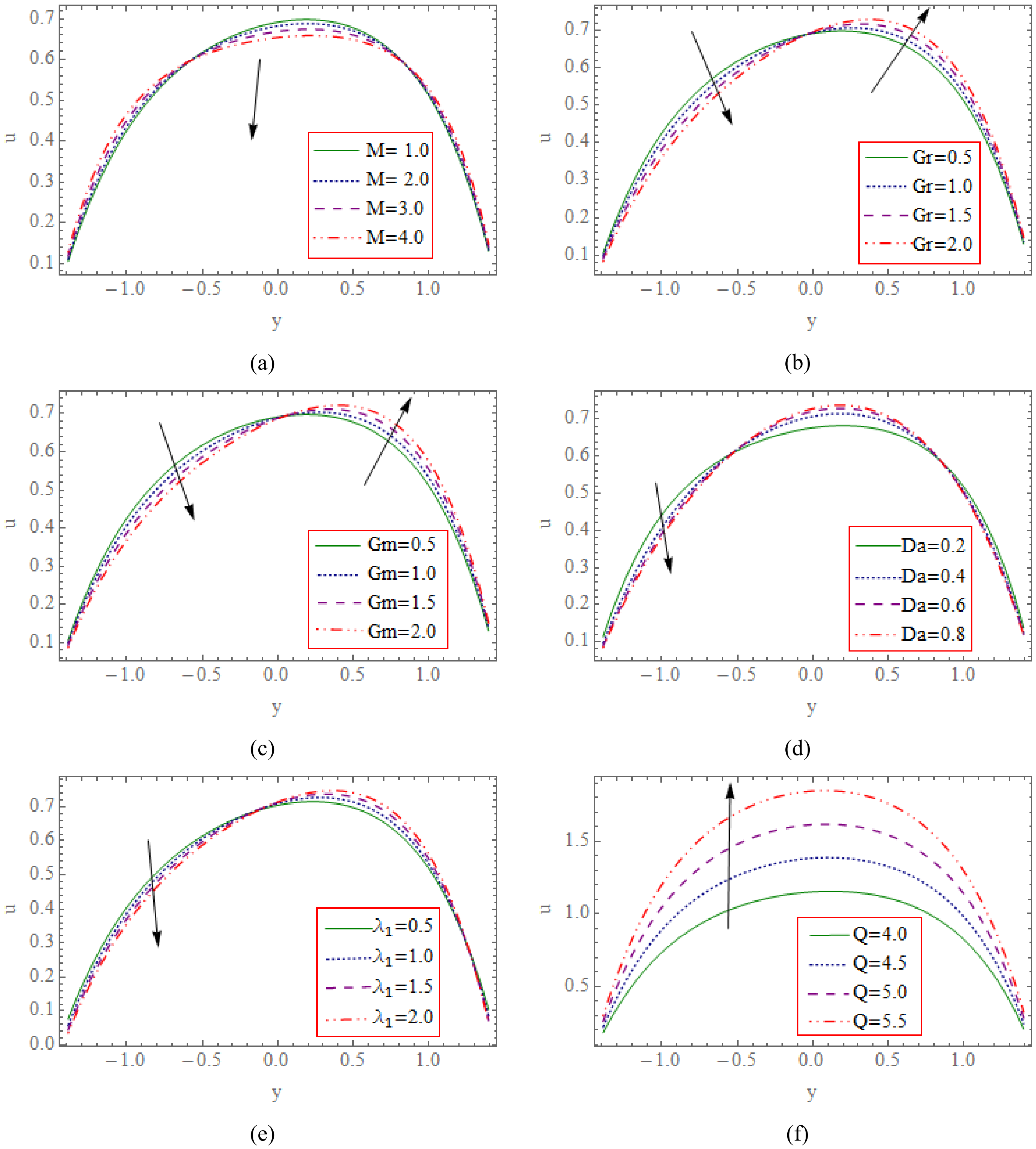

Figure 2. Velocity u versus y for: (a). M, (b). Gr, (c). Gm, (d). Da, (e). λ_1 and (f). Q when $x = 0.3,\ t = 0.1,\ a_1 = 0.1,\ a_2 = 0.1,\ Gr = 0.5,\ Gm = 0.5,\ Br = 0.1,\ Nt = 0.2,\ Nb = 0.2,\ Da = 0.3,\ M = 1.0,\ m = 0.3,\ \eta = \frac{\pi}{6},\ \lambda_1 = 0.1,\ k_1 = 1.0,\ \alpha_1 = 0.1,\ \alpha_2 = 0.1,\ \alpha_3 = 0.1,\ Pr = 0.7,\ d = 0.5,\ Q = 3.0.$

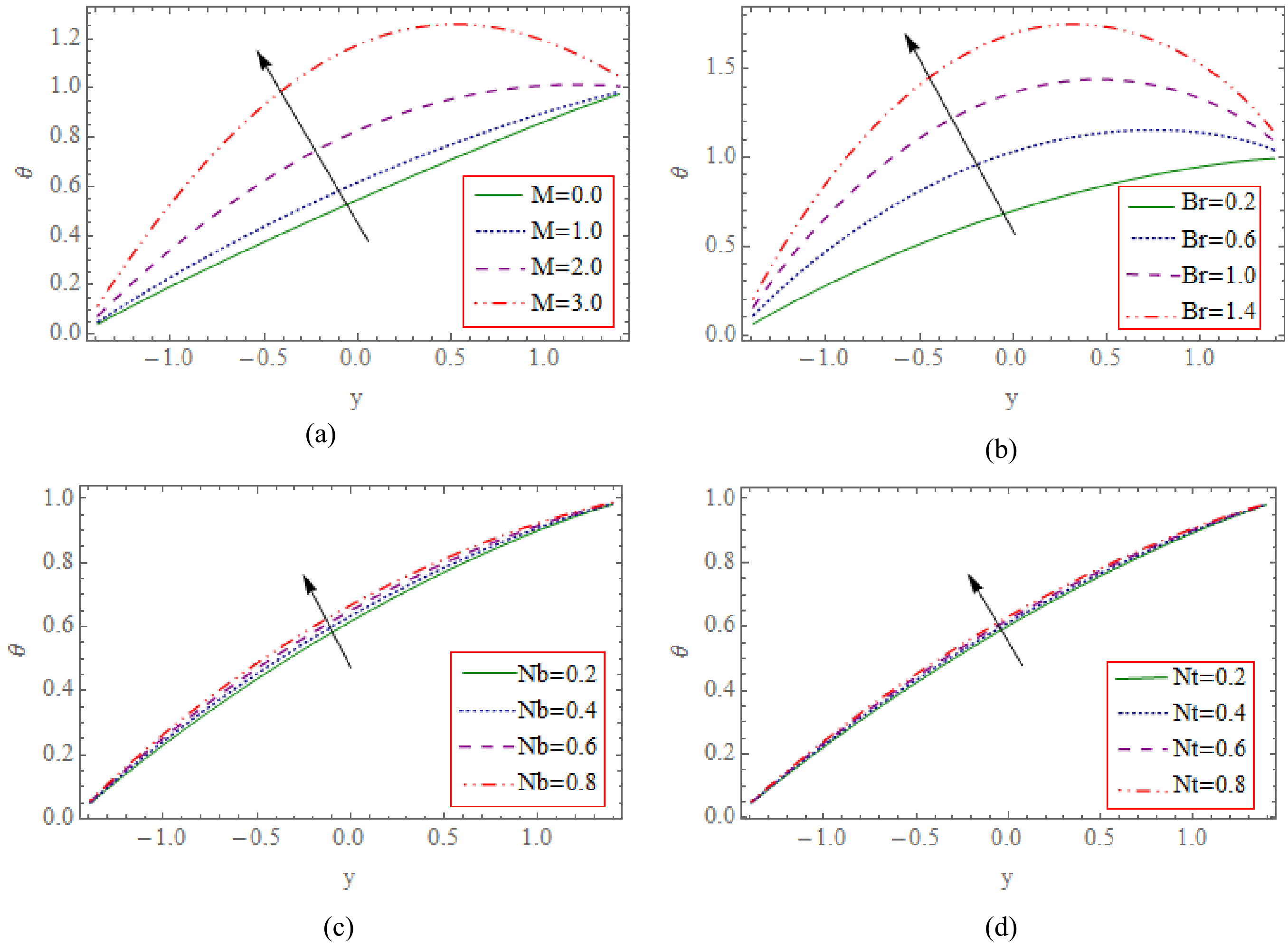

Figure 3. Temperature θ versus y for: (a). M, (b). Br, (c). Nb, (d). Nt when $x = 0.3,\ t = 0.1,\ a_1 = 0.1,\ a_2 = 0.1,\ Gr = 0.5,\ Gm = 0.5,\ Br = 0.1,\ Pr = 0.7,\ d = 0.5,\ Q = 3.0,\ Nt = 0.2,\ Nb = 0.2,\ Da = 0.3,\ M = 1.0,\ m = 0.3,\ \eta = \frac{\pi}{6},\ \lambda_1 = 0.1,\ k_1 = 1,\ \alpha_1 = 0.1,\ \alpha_2 = 0.1, \alpha_3 = 0.1$

Concentration ζ falls when the values of pertinent parameters M, Nt and Pr boost (see Figure 4(a), Figure 4(c) and Figure (4d)) and reverse pattern is seen for Nb (see Figure 4(b)). However, the concentration is not significantly affected by the Brownian motion parameter. The distribution of concentration also filfil the boundaryconditions. It is observed that, the embedded parameters behave in the exact opposite manner when we compared the temperature profile with regard to concentration distribution. Our findings for concentration profile are matched to those results for pertinent perameters reported in ref. [3].

For various values of the M, Br, Nt the heat transfer rate Z is displayed in Figure 5. We noticed that heat transfer coefficient Z rises with the increament in the value of M, Br. so, results are shown in figure 5(a) and figure 5(b). Similarly, heat transfer rate Z falls with the increase of Nt which is exposed in figure 5(c).The sinusoidal behaviour of heat transfer rate is observed.It is noticed that outlook of heat transfere rate is oscillatary. Our outcome for Br parameter is analogous to the upshot reported in ref [18].

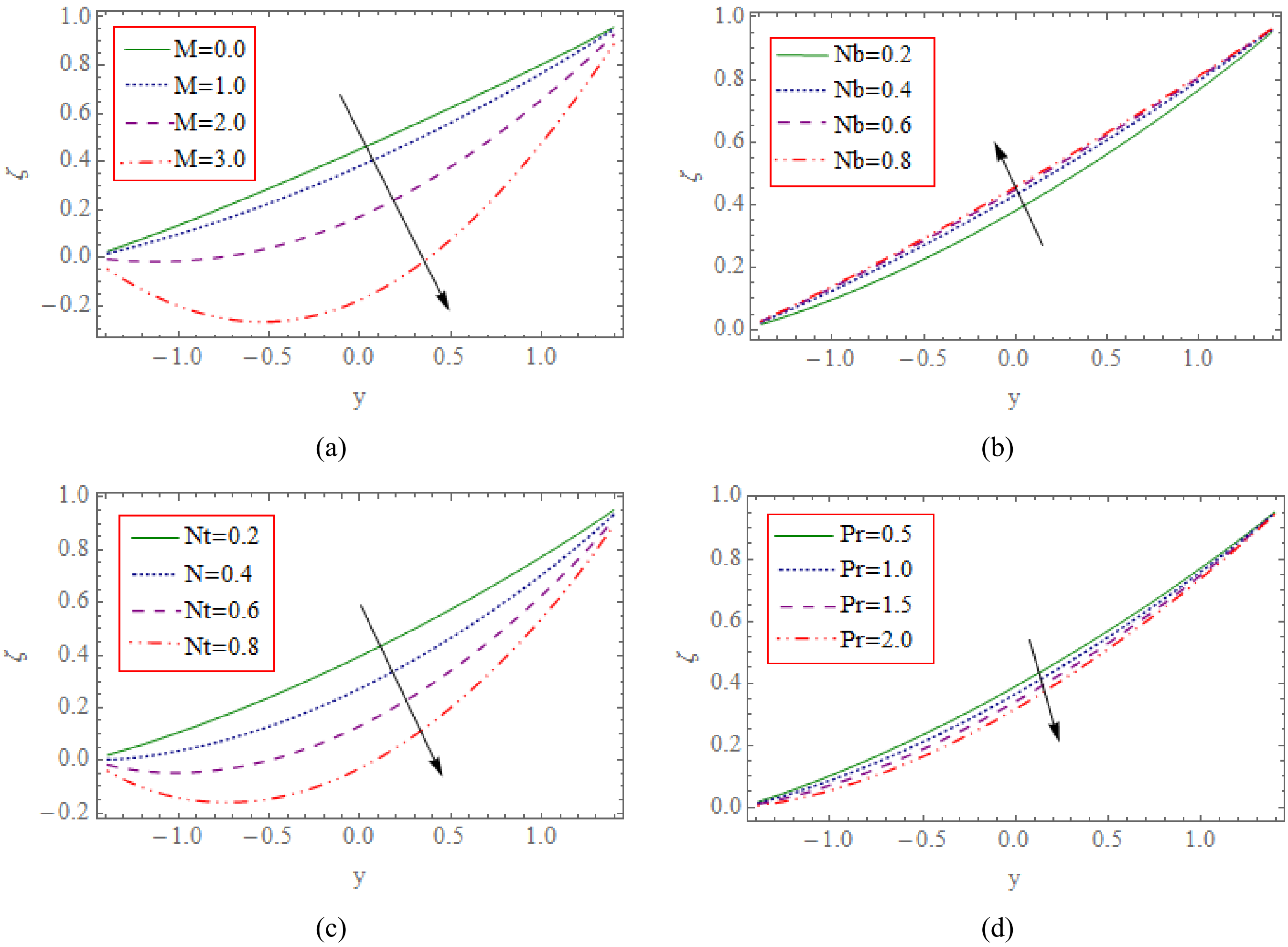

Figure 4. Concentration ζversus y for: (a). M, (b). Nb, (c). Nt and (d). Pr when $x = 0.3,\ t = 0.1,\ a_1 = 0.1, a_2 = 0.1,\ Gr = 0.5,\ Gm = 0.5,\ Br = 0.1,\ Pr = 0.7,\ d = 0.5,\ Q = 3.0,\ Nt = 0.2,\ Nb = 0.2,\ Da = 0.3,\ M = 1.0,\ m = 0.3,\ \eta = \frac{\pi}{6},\ \lambda_1 = 0.1,\ k_1 = 1, \alpha_1 = 0.1, \alpha_2 = 0.1, \alpha_3 = 0.1$.

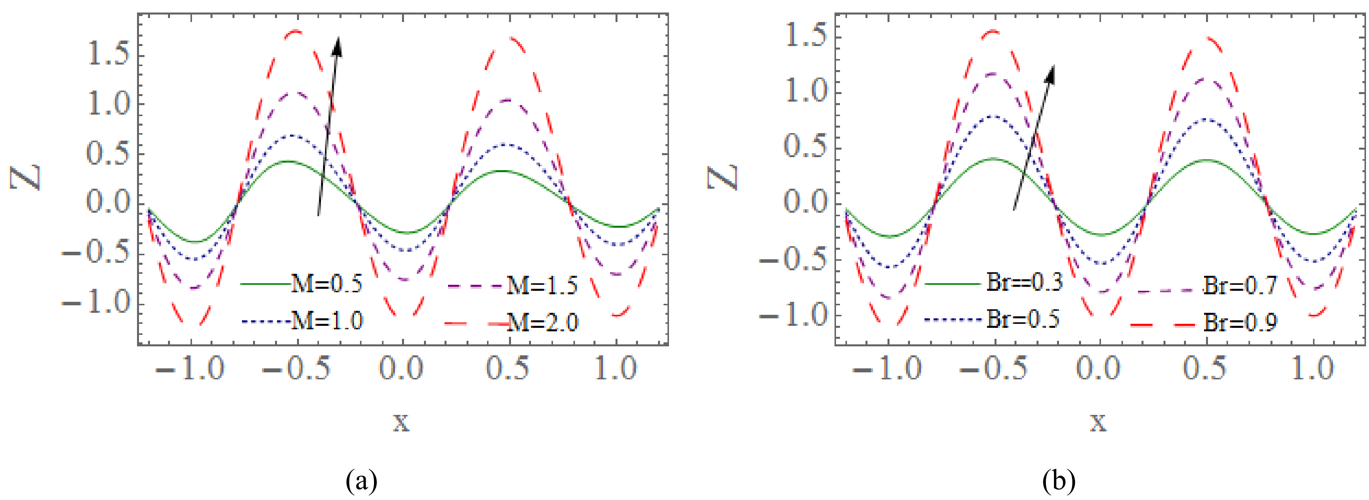

Figure 5. Heat transfer rate Z versus x for: (a) M, (b) Br, when $x = 0.3,\ t = 0.5,\ a_1 = 0.08,\ a_2 = 0.08,\ Gr = 0.5,\ Gm = 0.5,\ Br = 1,\ Pr = 0.8,\ d = 0.5,\ Q = 3.0,\ Nt = 0.5,\ Nb = 0.5,\ Da = 0.5,\ M = 2.0,\ m = 0.3,\ \eta = \frac{\pi}{6},\ \lambda_1 = 0.1,\ k_1 = 0.1,\ \alpha_1 = 0.1, \alpha_2 = 0.1, \alpha_3 = 0.1$

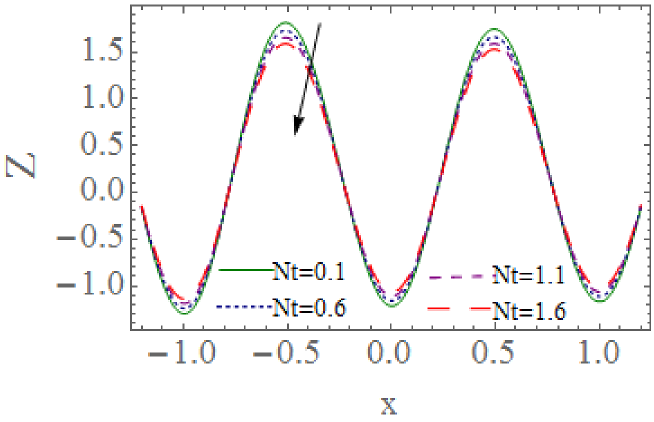

Figure 5 (c). Heat transfer rate Z versus x for Nt

6. Conclusion

In this research, we addressed on the inclined Magnetohydrodynamics (MHD) effects in a tapered asymmetric porous channel with peristalsis under the effects of slip boundary conditions. From present study, we concluded that fluid velocity declines in the channel's central portion whilst boosted up near the walls under a stronger magnetic field parameter. Because greater Hartman number strengthen theresistive force (Lorentz force) that opposes fluid velocity. For escalating levels of Gm and Gr the fluid viscosity decays and in view of this fact the dual response of velocity is captured.Temperature goes up whilst concentration decays for increament in values of M. It happens due to the increament in magnetic field. Growing value of Br enhances the temperature profile owing to the effects of viscous dissipation. A rise in Nt and Nb represents an increament in temperature which is consistent with the nanoparticles' effective transfer from the wall to the fluid, causing a notable boost in the temperature profile.It is revealed that outlook of heat transfer rate Z is oscillatory because of the contraction and expansion of the walls of the channel. The absolute value of heat transfer rate Z enhances when M and Br goes up and contrary trend is demonstrated for Nt.

Competing Interest Statement

The authors declare no known competing financial interests or personal relationships that could have influenced the work reported in this paper.

Data and Materials Accessibility

No data or additional materials were utilized for the research described in the article.

References

[1] M. Nazeer, M.I. Khan, M.U. Rafiq, N.B. Khan, "Numerical and scale analysis of Eyring-Powell nanofluid towards a magnetized stretched Riga surface with entropy generation and internal resistance,'' International Communications in Heat and Mass Transfer, 119, 104968, 2020.

[2] Y.M. Chu, F. Ahmad, M.I. Khan, M. Nazeer, F. Hussain, N.B. Khan, L, Mei, "Numerical and scale analysis of non-Newtonian fluid (Eyring-Powell) through pseudo-spectral collocation method (PSCM) towards a magnetized stretchable Riga surface,'' *Alexandria Engineering Journal,* 60(2), pp. 2127-2137, 2021.

[3] M. Rafiq, M. Sajid, S.E. Alhazmi, M.I. Khan, E.R. El-Zahar, "MHD electroosmotic peristaltic flow of Jeffrey nanofluid with slip conditions and chemical reaction,'' *Alexandria Engineering Journal,* 61(12), pp. 9977-9992, 2022.

[4] B.B. Divya, G. Manjunatha, C. Rajashekhar, H. Vaidya, K.V. Prasad, "Effects of inclined magnetic field and porous medium on peristaltic flow of a Bingham fluid with heat transfer,'' *Journal of Applied and Computational Mechanics,* 7(4), pp. 1892-1906, 2021.

[5] A.M. Abd-Alla, S. M. Abo-Dahab, E. N. Thabet, M. A. Abdelhafez, "Impact of inclined magnetic field on peristaltic flow of blood fluid in an inclined asymmetric channel in the presence of heat and mass transfer,'' Waves in Random and Complex Media, pp. 1-25, 2022.

[6] A.M. Abd-Alla, E.N. Thabet, F.S. Bayones, "Numerical solution for MHD peristaltic transport in an inclined nanofluid symmetric channel with porous medium,'' *Scientific Reports,* 12(1), pp. 1-11, 2022.

[7] N.B. Naduvinamani, A.S. Guttedar, L. Devindrappa, "On the Magnetohydrodynamic (MHD) Peristaltic Flow of a Hyperbolic Tangent Fluid in a Tapered Asymmetric Channel,'' *Journal of Nanofluids,* 11(5), pp. 737-744, 2022.

[8] M. Devakar, K. Ramesh, K. Vajravelu, "Magnetohydrodynamic effects on the peristaltic flow of couple stress fluid in an inclined tube with endoscope,'' *Journal of Computational Mathematics and Data Science,* 2, 100025, 2022

[9] F.S. Bayones, A.M. Abd-Alla, E.N. Thabet, "Magnetized dissipative Soret effect on nonlinear radiative Maxwell nanofluid flow with porosity, chemical reaction and

Joule heating,'' *Waves in Random and Complex Media,* pp. 1-19, 2022.

[10] T.W. Latham, "Fluid motions in a peristaltic pump (Doctoral dissertation,'' *Massachusetts Institute of Technology).* 1966.

[11] A.H. Shapiro, M.Y. Jaffrin, S.L. Weinberg, "Peristaltic pumping with long wavelengths at low Reynolds number,'' *Journal of fluid mechanics,* 37(4), pp. 799-825, 1969.

[12] Z. Hussain, k. Al-Khaled, U. Ashrif, A. Abbasi, S.U. Khan, W. Farooq, M.Y. Malik, "A mathematical model for radiative peristaltic flow of Jeffrey fluid in curved channel with Joule heating and different walls: Shooting technique analysis,'' *Ain Shams Engineering Journal,* 13(5), 101685, 2022

.[13] T. Hayat, S. Farooq, B. Ahmad, A. Alsaedi, "Effectiveness of entropy generation and energy transfer on peristaltic flow of Jeffrey material with Darcy resistance,'' *International Journal of Heat and Mass Transfer,* 106, pp. 244-252. 2017.

[14] A.M. Abd-Alla, E.N. Thabet, F.S. Bayones, A.M. Alsharif, "Heat transfer in a non-uniform channel on MHD peristaltic flow of a fractional Jeffrey model via porous medium,'' *Indian Journal of Physics,* pp. 1-11, 2022.

[15] M.I. Khan, M. Lashin, N.B. Khedher, B. Ahmed, S.U. Khan, M. Oreijah, A.M. Galal, "Peristaltic Phenomenon in an Asymmetric Channel Subject to Inclined Magnetic Force and Porous Space,'' *Bioengineering,* 9(10), 588, 2022.

[16] A.M. Abd-Alla, R.A. Mohamed, S.M. Abo-Dahab, M. S. Soliman, "Rotation, initial stress effect on MHD peristaltic flow of reacting radiating fourth-grade nanofluid with viscous dissipation and Joule heating,'' *Waves in Random and Complex Media,* pp. 1-35, 2022.

[17] Z. Asghar, M.W. Saeed Khan, M.A. Gondal and A. Ghaffari," Channel flow of non-Newtonian fluid due to peristalsis under external electric and magnetic field,'' Proceedings of the Institution of Mechanical Engineers, Part E: *Journal of Process Mechanical Engineering,* 09544089221097693, 2022.

[18] A. Tanveer, S. Mahmood, T. Hayat, A. Alsaedi, "On electroosmosis in peristaltic activity of MHD non-Newtonian fluid," *Alexandria Engineering Journal,* 60(3), pp. 3369-3377, 2021.

[19] N. Ammar, H.A. Ali, "Mathematical modeling for peristaltic transport of non-Newtonian fluid through inclined non-uniform channel under the effect of surface roughness," *International Journal of Nonlinear Analysis and Applications,* 13(2), pp. 117-130, 2022.

[20] M. Kahshan, D. Lu, A.M. Siddiqui, "A Jeffrey fluid model for a porous-walled channel: Application to flat plate dialyzer,'' *Scientific reports,* 9(1), pp. 1-18, 2019.

[21] F. Ali, S. Murtaza, I. Khan, N.A. Sheikh, and K. S, "Atangana–Baleanu fractional model for the flow of Jeffrey nanofluid with diffusion-thermo effects: applications in engine oil, Advances in Difference Equations," pp. 1-21, 2019.

[22] A.S. Kotnurkar, J. Beleri, I.A. Badruddin, N.A. Ahammad, "Effect of Thermal Radiation and Double-Diffusion Convective Peristaltic Flow of a Magneto-Jeffrey Nanofluid through a Flexible Channel," *Mathematics,* 10(10), 170, 2022.

[23] A.S. Kotnurkar, V.T. Talawar, "Influence of thermal jump and inclined magnetic field on peristaltic transport of Jeffrey fluid with silver nanoparticle in the eccentric annulus. Heliyon,'' 8(9), e10543, 2022.

[24] M. Rafiq, M. Sajid, S.E. Alhazmi, M.I. Khan, E.R. El-Zahar, "MHD electroosmotic peristaltic flow of Jeffrey nanofluid with slip conditions and chemical reaction,'' *Alexandria Engineering Journal,* 61(12), pp. 9977-9992, 2022.

[25] P.P. Singh, G. Kumar, S. Raghav, "Peristaltic Flow of Jeffrey Fluid through a slanted cylinder,'' *JOURNAL OF ALGEBRAIC STATISTICS,* 13(2), pp. 3689-3695, 2022.

[26] S. Bajwa, S. Ullah, A.S. Al-Johani, I. Khan, M. Andualem, "Effects of MHD and Porosity on Jeffrey Fluid Flow with Wall Transpiration,'' *Mathematical Problems in Engineering*, 2022

[27] M. Aleem, M.I. Asjad, A. Ahmadian, M. Salimi, M. Ferrara, "Heat transfer analysis of channel flow of MHD Jeffrey fluid subject to generalized boundary conditions,'' *The European physical journal plus*, 135(1), pp. 1-15, 2020.

[28] Z. Hussain, K. Al-Khaled, U. Ashrif, A. Abbasi, S.U. Khan, W. Farooq, and M. Y. Malik, "A mathematical model for radiative peristaltic flow of Jeffrey fluid in curved channel with Joule heating and different walls: Shooting technique analysis,'' *Ain Shams Engineering Journal,* 13(5), 101685, 2022

[29] A.S. Kotnurkar, V.T. Talawar, "Influence of thermal jump and inclined magnetic field on peristaltic transport of Jeffrey fluid with silver nanoparticle in the eccentric annulus,'' Heliyon, 8(9), e10543, 2022

[30] A.M. Abd-Alla, S.M. Abo-Dahab, M.A. Abdelhafez, E.N. Thabet, "Effects of heat transfer and the endoscope on Jeffrey fluid peristaltic flow in tubes,'' *Multidiscipline Modeling in Materials and Structures,* 17(5), pp. 895-914, 2021.

[31] H. Vaidya, C. Rajashekhar, B.B. Divya, G. Manjunatha, K.V. Prasad, I.L. Animasaun, "Influence of transport

properties on the peristaltic MHD Jeffrey fluid flow through a porous asymmetric tapered channel," Results in Physics, 18, 103295, 2020.

[32] J. Wang, H. Deng, Z. Tao, Y. Li, J. Zhu, "Heat transfer in a rotating rectangular channel with impingement jet and film holes,'' *International Journal of Thermal Sciences,* 163, 106832, 2021

[33] R. Vinoth, B. Sachuthananthan, "Flow and heat transfer behavior of hybrid nanofluid through microchannel with two different channels,'' *International Communications in Heat and Mass Transfer*, 123, 105194, 2021.

[34] W. Abbas, N. Eldabe, S. Marzouk," Soret and Dufour effects with Hall currents on peristaltic flow of Casson fluid with heat and mass transfer through non-Darcy porous medium inside vertical channel,'' *Egyptian Journal of Chemistry,* 64(9), pp. 5215-5225, 2021.

[35] S. Nazir, M. Kashif, A. Zeeshan, H. Alsulami, M. Ghamkhar, "A study of heat and mass transfer of non-Newtonian fluid with surface chemical reaction, *"Journal of the Indian Chemical Society*, 99(5), 100434, 2022.

[36] A. M. Abd-Alla, S. M. Abo-Dahab, E. N. Thabet, M.A. Abdelhafez, "Heat and mass transfer for MHD peristaltic flow in a micropolar nanofluid: mathematical model with thermophysical features," *Scientific Reports,* 12(1), 21540, 2022.

[37] F. Hussain, ''Heat and Mass Transfer Analysis in MHD Peristaltic Flow of Newtonian and Non-Newtonian Fluids bounded with Porous Tilted Channel," 2022.

[38] A.M. Abd-Alla, S.M. Abo-Dahab, E.N. Thabet, M.A. (Abdelhafez), "Peristaltic pump with heat and mass transfer of a fractional second grade fluid through porous medium inside a tube. *Scientific reports*," 12(1), pp. 1-14, 2022.

[39] A.M. Abd-Alla, S.M. Abo-Dahab, E.N. Thabet, M.A. (Abdelhafez), F.S. Bayones, "Heat and mass transfer in a peristaltic rotating frame Jeffrey fluid via porous medium with chemical reaction and wall properties*,"* *Alexandria Engineering Journal*, 2022.

[40] A. Salmi, H.A. Madkhali, B. Ali, M. Nawaz, S.O. Alharbi, A.S. Alqahtani, "Numerical study of heat and mass transfer enhancement in Prandtl fluid MHD flow using Cattaneo-Christov heat flux theory," *Case Studies in Thermal Engineering,* 33, 101949, 2022.

[41] A. Tanveer, S. Mahmood, T. Hayat, A. Alsaedi, "On electroosmosis in peristaltic activity of MHD non-Newtonian fluid*," Alexandria Engineering Journal,* 60(3), pp. 3369-3377, 2021.

[42] F.S. Bayones, A. M. Abd-Alla, E. N. Thabet, "Effect of heat and mass transfer and magnetic field on peristaltic flow of a fractional Maxwell fluid in a tube," *Complexity*, pp. 1-12, 2021.

[43] A. M. Abd-Alla, S.M. Abo-Dahab, E.N. Thabet, M.A. Abdelhafez, "Heat and mass transfer for MHD peristaltic flow in a micropolar nanofluid: mathematical model with thermophysical features," *Scientific Reports,* 12(1), 21540, 2022.

[44] M.V. Krishna, B.V. Swarnalathamma, "Heat and mass transfer on the Peristaltic flow of an incompressible electrically conducting Williamson fluid through a porous medium in a symmetric channel with Hall current effects and inclined magnetic field," *International Journal of Scientific Engineering and Research*, 6(9), pp. 941-957, 2019,

[44] H. Yasmin, N. Iqbal, A. Tanveer,"Engineering applications of peristaltic fluid flow with hall current, thermal deposition and convective conditions," Mathematics, 8(10), 1710, 2020.

[45] Z. Abbas, M.Y. Rafiq, S. Khaliq, A. Ali, "Dynamics of the thermally radiative and chemically reactive flow of Sisko fluid in a tapered channel,*" Advances in Mechanical Engineering,* 14(10), 16878132221129735, 2022.